

# Simulation of the COVID-19 pandemic on the social network of Slovenia: estimating the intrinsic forecast uncertainty

Žiga Zaplotnik, Aleksandar Gavrič, Luka Medic

May 28, 2020

## Abstract

In the article a virus transmission model is constructed on a simplified social network. The social network consists of more than 2 million nodes, each representing an inhabitant of Slovenia. The nodes are organised and interconnected according to the real household and elderly-care center distribution, while their connections outside these clusters are semi-randomly distributed and fully-linked. The virus spread model is coupled to the disease progression model. The ensemble approach with the perturbed transmission and disease parameters is used to quantify the ensemble spread, a proxy for the forecast uncertainty.

The presented ongoing forecasts of COVID-19 epidemic in Slovenia are compared with the collected Slovenian data. Results show that infection is currently twice more likely to transmit within households/elderly care centers than outside them. We use an ensemble of simulations ( $N = 1000$ ) to inversely obtain posterior distributions of model parameters and to estimate the COVID-19 forecast uncertainty. We found that in the uncontrolled epidemic, the intrinsic uncertainty mostly originates from the uncertainty of the virus biology, i.e. its reproductive number. In the controlled epidemic with low ratio of infected population, the randomness of the social network becomes the major source of forecast uncertainty, particularly for the short-range forecasts. Social-network-based models are thus essential for improving epidemics forecasting.

## 1 Introduction

The ongoing COVID-19 epidemic has revealed a major gap in our ability to forecast the evolution of the epidemic. There are several ways to simulate the epidemic dynamics. The most common approach is using compartmental models of susceptible (S), immune (I), recovered (R) population, i.e. SIR models [1, 2]. These are described by a system of differential equations given some predefined parameters, such as probability of the disease transmission and the rate of recovery or mortality. Another variation of the SIR model is a SEIR model, which accounts also for the exposed (E) population, representing infected but not yet infectious subjects. The SEIR model is combined with activation functions to smoothly model social factors affecting virus spread and the disease progression. A major setback of the deterministic epidemic models is that they are only applicable for sufficiently large populations, where the assumption of homogeneous spread of the virus is valid [3]. For coronaviruses, there is evidence that some infectious cases, the so called superspreaders, spread virus more than others [4]. Their role is of the utmost importance in the initial uncontrolled phase of an epidemic and in its final controlled phase with low population of infected. Thus, deterministic SEIR models are also unable to properly describe the intrinsic uncertainty of the virus spread due to heterogeneous connectivity of the social network and due to heterogeneous disease progress of the infected population.

Consequently, we use node-based approach [5] to simulate the SARS-CoV-2 coronavirus spread over a simplified social network of more than 2 million nodes with a total of up to 20 million connections, representing the population of Slovenia and the connections of its inhabitants, with realistic distinction between household and outer connections. Despite being computationally more expensive, an advantage of network approach is that it allows direct simulation of intervention

$k$ persons in household	number of $k$ -person households
1	269898
2	209573
3	152959
4	122195
5	43327
6	17398
7	6073
8	3195
25	100 care centers with 8 groups each

Table 1: Households distribution in Slovenia, based on the data of Statistical Office of Republic of Slovenia [7].

measures as well as planning of the future strategies of the the virus containment [e.g. 6] and lockdown-exit strategy. Here, we combine the network approach together with an ensemble-of-simulations approach which allows to estimate the uncertainty of the predictions which stems from the randomized network, initial number of infected, and the uncertainty of the coronavirus transmission parameters and disease progress parameters.

Section 2 describes the social network model, the virus transmission model and the coupled disease progression model. The probabilistic ensemble forecast of the COVID-19 pandemic for Slovenia and the contribution of different model components to the total forecast uncertainty is described in Section 3. Discussion, conclusions and further outlook are given in Section 4.

## 2 Methodology

### 2.1 Social network model

The social network model of the population of Slovenia distinguishes household connections and connections outside households. A total of  $N = 2045795$  nodes is used in the social network. The number of  $k$ -person households is given in Table 1. There are approximately 100 elderly care centers in Slovenia with a total of approximately 20000 residents. Each elderly care center is assumed to include 8 distinct groups of 25 people. Average household/care group consists of 2.5 people in Slovenia so the average number of contacts per person within household is 1.5.

In normal conditions, contact number distribution follows power law with fat tails [8], which are associated with superspreader events, e.g. large public gatherings such as sport and cultural events. However, since all public events are canceled in the event of the COVID-19 epidemic, these fat tails are cut off [9] and the topology of the social network changes substantially. In conditions without large public gatherings, it is reasonable to assume that certain people still have much larger number of contacts than others. The studies of social mixing, e.g. POLYMOD study of social interactions within 8 European countries, typically report negative binomial distribution of the number of contacts [10, 11]. We assumed mean number of contacts outside households to be 13.5 with standard deviation of 10.5. Instead of negative binomial distribution, we rather use smooth gamma distribution, which resembles the shape of the binomial distribution but has some useful mathematical properties, which will be exploited in the continuation. Thus, we model the connectivity, i.e. the number of contacts per person, using the gamma probability distribution, which is essentially an exponential distribution

$$p(x; k, \theta) = \frac{1}{\Gamma(k)\theta^k} x^{k-1} e^{-\frac{x}{\theta}}. \quad (1)$$

In this study, we use  $k = 1.65$  and  $\theta = 4.08$  for the initial setup, which gives an average number of 13.5 contacts per person per day (Fig. 1). Together with 1.5 family contacts per person per day,

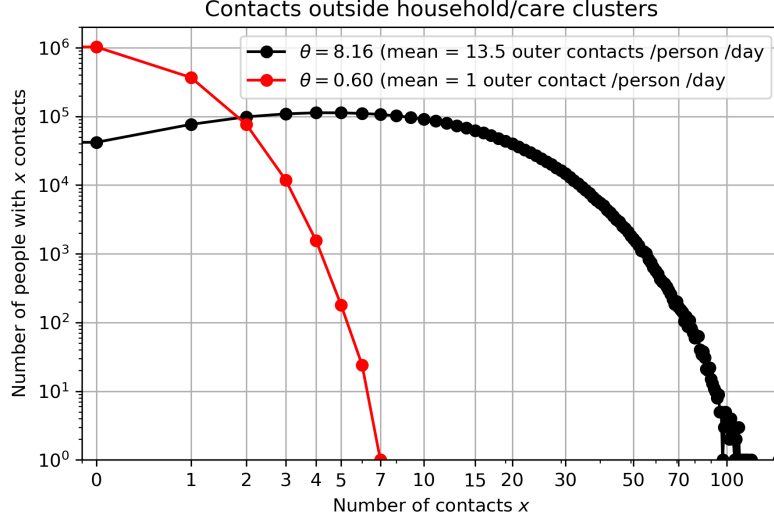


Figure 1: Number distribution  $N(x) = p(x)N$  by the number of contacts in the social network model. The black graph shows the assumed distribution of people with a given number of outer contacts in a normal, non-epidemic, phase, while the red graph presents reduced number of outer contacts in the case of a social distancing measures.

the total number of contacts per person per day is 15. Here, we assume that the average number of contacts is the same for each age group, despite studies showing that elderly have reduced number of contacts [12]. The average contact number per person per day varies for different countries [11], however 15 contacts per day is a reasonable guess for Slovenia. We also assume quasi-static social network, i.e. only 20% of contacts are new every day, and the remaining 80% are static. This choice is a first guess, justified by the fact that only around 20% of all daily contacts last less than 15 minutes [11]. These can be regarded as random sporadic contacts. Self-distancing measures to mitigate COVID-19 can be imposed by decreasing parameter  $\theta$ , which also decreases the average number of outer contacts (Fig. 1).

Fig. 2 shows an example of the connectivity change of a minimised network with 88 nodes clustered on a circle with the real household distribution taken into account.

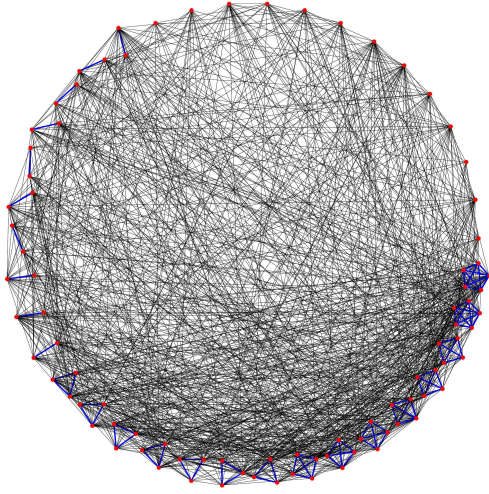
Technically, we connect the graph in the following way:

1. number of outer contacts for each node is randomly drawn from Gamma distribution (1). If node  $i$  has  $x_i = 0.33$  contacts per day, it means that it will have 0 contacts 2/3 of the time and 1 contact 1/3 of the time of the simulation;
2. for each node  $i$ , we randomly assign the connections to  $x_i$  other nodes, where  $x_i$  is the number of contacts of node  $i$ . However, not every node has the same probability of being picked as a neighbour. Node  $j$ , which has  $x_j$  contacts, is picked as a neighbour with probability  $x_j N(x_j) / T$ , where  $N(x_j)$  is the number of nodes with  $x_j$  contacts and  $T$  is the total number of contacts in the network ( $T$  is twofold the number of connections). Sampling over Gamma distribution (1) gives us a distribution of  $N(x) = p(x)N$ . When picking the neighbours, we actually sample the same Gamma distribution times  $x$ , i.e.

$$p_n(x) = p(x; k, \theta)x = \frac{1}{\Gamma(k)\theta^k} x^k e^{-\frac{x}{\theta}} \propto p(x; k+1, \theta). \quad (2)$$

3. The shape of the social network is changing (80% of connections static, 20% changing) at every timestep of the simulation to account for random sporadic contacts. (a) The number of contacts of node  $i$  is fixed (randomly jumps between  $\lfloor x_i \rfloor$  and  $\lceil x_i \rceil$  based on the value of  $x_i$ ). For example, if a node has 0.33 contacts per day, 1 contact is picked with probability

a)



b)

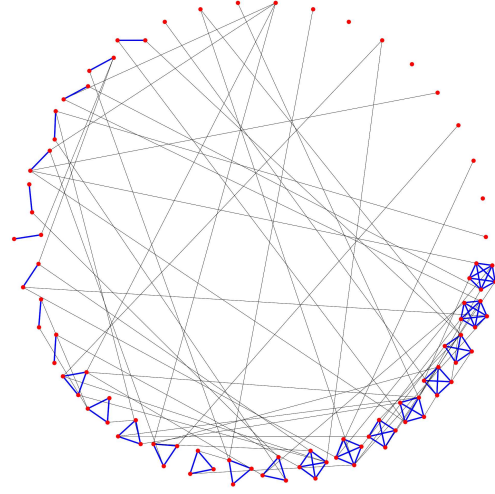


Figure 2: Connectivity of the social network of  $N = 88$  nodes for a) densely connected graph, where each node has on average 15 contacts per day (1.5 family and 13.5 outer contacts,  $\theta = 22.5$ ) and b) sparsely connected graph, where each node has on average 2.5 contacts per day (1.5 family and 1 outer contact). Red dots are nodes, blue lines represents household connections and black lines outer connections. The graph represents a minimized version of the social network used in the virus spread simulation.

1/3 and 0 contacts with probability 2/3. (b) The social network is partially rewired at every timestep to account for superspreaders mobility.

An important advantage of our network approach is that the nodes are not connected randomly through “half-links” (directed connections linking egos to their contacts, the alters) [13, 14], such as in the vast majority of modelling studies, where the WAIFW (who-acquires-infection-from-whom) matrices were constructed based on the egocentric data. Instead, nodes are fully-linked.

### 2.1.1 Compartments

Similarly as in the deterministic SEIR model, we divided the population into compartments, where we used the following compartmental division: susceptible, infected, infectious (exposed), hospitalised with severe illness, hospitalised and critically ill (ICU treatment), hospitalised and fatal, and recovered. The latter are assumed to be immune for the whole simulation period. In the network model, a susceptible node becomes exposed (infected) with a certain probability (called an attack rate) when in contact with an infectious node. After a certain period of time, the infected node progresses into infectious state. In the accordance with the chosen compartmental division we monitor each node by adapting its clinical state at every timestep. Since all the periods are stochastic variables, e.g. infectious and recovery periods, those periods widely vary among the nodes (and the variations would be even greater if we would account for the demographic properties, e.g. age and sex).

## 2.2 Virus transmission model

### 2.2.1 Reproduction number $R_0$

A basic reproduction number,  $R_0$ , provides information on the average speed of virus transmission in an uncontrolled phase of the epidemic. Different methodologies produced different results,

however the majority of reported  $R_0$  for SARS-CoV-2 is within 2 and 3. Here, we use median reported  $R_0$  from a number of studies, as well as its median confidence intervals, i.e.  $R_0 = 2.68$ , with 95% confidence interval  $[2, 3.9]$ . This approach is not the optimal one, since we are trading accuracy for precision. The published  $R_0$  values as well as our deduced  $R_0$  distribution is shown in Fig. 3a,b. The optimal log-normal distribution should thus match the following conditions:  $\text{CDF}(R_0^L; \mu, \sigma, \Delta x) = 0.025$ ,  $\text{CDF}(R_0^U; \mu, \sigma, \Delta x) = 0.975$ , and  $\text{median}(\text{CDF}) = R_0$ , where  $R_0^L$  and  $R_0^H$  are lower and upper boundaries of  $R_0$ , CDF stands for log-normal cumulative distribution function and its median is  $\exp(\mu)$ . Then, we define a quadratic cost function, which includes all the above criteria, and by minimizing it, we obtain the optimal parameters for log-normal distribution:  $\Delta x = 0.36$ ,  $\sigma = 1.14$ ,  $\exp \mu = 1.54$ .

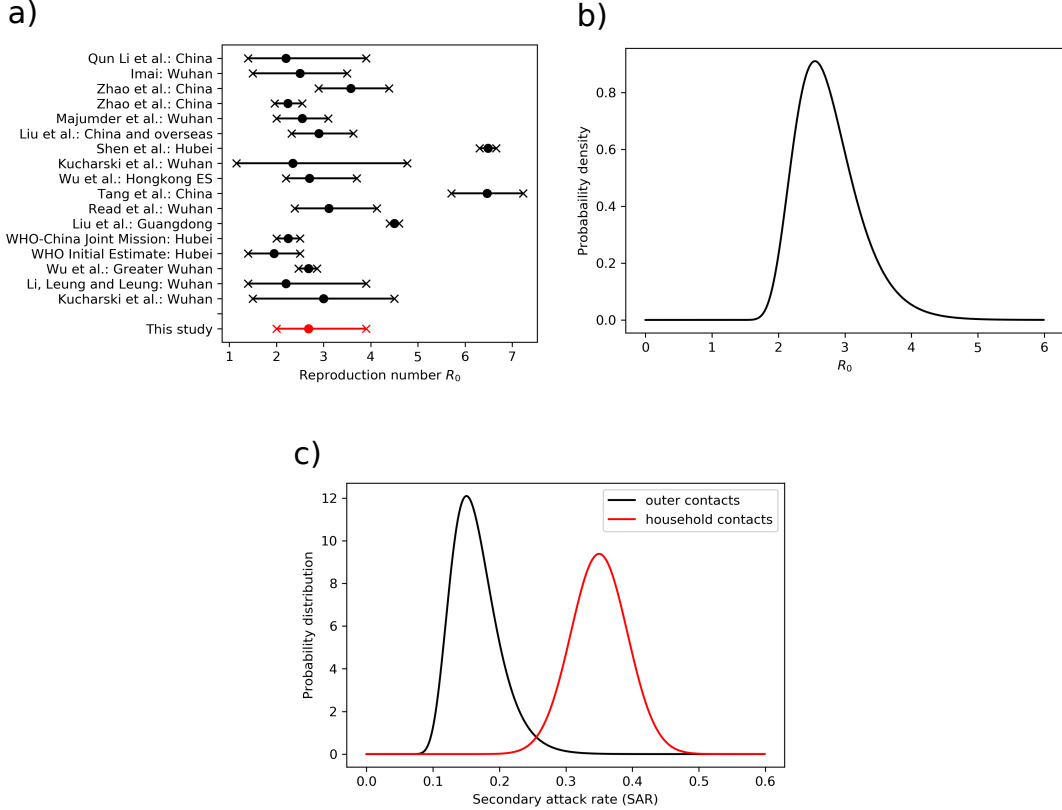


Figure 3: a) Basic reproduction number  $R_0$  (median and 95% confidence interval), reported in a number of studies for different locations [15, 16, 17, 18, 19, 20, 21, 22, 23, 24, 25] and references therein. b) Log-normal probability density function of the basic reproduction number, used for ensemble simulations. c) Probability distribution of secondary attack rates for household contacts and outer contacts.

### 2.2.2 Attack rate

In general, the basic reproduction number,  $R_0$  can be decomposed into the secondary attack rate times the number of contacts. The secondary attack rate ( $SAR$ ) is defined as the probability that an infection occurs among susceptible people within a specific group (i.e. household contacts or other contacts outside households). The measure can provide an indication of how social interactions relate to the transmission risk. We can further decompose the  $R_0$  into the household risk of infection and outer risk of infection (following [26])

$$R_0 = SAR_h N_h + SAR_c N_c, \quad (3)$$

where  $SAR_h$  and  $SAR_c$  are secondary attack rates within household and outside household (outer contacts), respectively.  $N_h$  and  $N_c$  are the numbers of household contacts and outer contacts. Here, one must notice that the above estimation of  $SAR_h$  assumed homogeneous mixing, while the network model is heterogeneous with  $R_0 = SAR_h(\langle N_h \rangle + \text{Var}(N_h)/\langle N_h \rangle) + SAR_c(\langle N_c \rangle + \text{Var}(N_c)/\langle N_c \rangle)$ . To be consistent with Liu et al. [26], we stick with formulation (3).

The study of Liu et al. [26] suggest  $SAR_h$  value of 35% (95% CI 27-44%) for SARS-CoV-2.  $SAR_h$  is almost normally distributed with mean 35% and  $2\sigma \approx 8.5$ . The distribution of  $R_0$  is given in the previous paragraph. It holds:  $SAR_c = (R_0 - SAR_h N_h)/N_c$ . This gives a transmission efficiency of  $SAR_c = 16\%$  (95% CI 10.8-25.1%). Fig. 3c shows probability distributions of secondary attack rates as used in the ensemble of simulations.

If the social infectious period is  $T_{inf} \approx 5$  days (check subsection 2.3.4), we can assume that the daily risk of getting infected from a certain household member is  $SAR_{h,daily}$  where  $1 - (1 - SAR_{h,daily})^{T_{inf}} = SAR_h$  and

$$SAR_{h,daily} = 1 - \exp\left(\frac{\ln(1 - SAR_h)}{T_{inf}}\right) \quad (4)$$

being equal 8.3% (95% CI 6.1-10.9%). Similarly, we compute  $SAR_{c,daily} = 3.4\%$  (95% CI 2.3-5.6%).

Some studies [e.g. 27] have concentrated only on the symptomatic secondary attack rates and have shown relatively smaller numbers: 0.45% (CI=0.12%-1.6%) among all close contacts and 10.5% (CI=0.12%-1.6%) among household members. However, these numbers cannot reproduce the reported  $R_0$  between 2 and 3.9 with any realistic number of contacts. Another study shows similar attack rates to what we use here [28].

The attack rate affects the virus transmission as follows. At each timestep of the simulation (every 1 day), the susceptible contacts of each infectious individual are randomly infected with probability  $SAR_{h,daily}$  or  $SAR_{c,daily}$ , depending whether the contact occurs within household or outside it.

## 2.3 Disease progression model

A simplified sketch of the disease progression model is shown in Fig. 4a. When a certain individual (node) gets infected, incubation period starts and several days will pass until the symptom onset. The majority of the infected people recovers at home, some die at home, while certain individuals are admitted to hospital in the following days. Several outcomes are possible: recovery after normal hospitalisation, recovery after intensive care unit hospitalisation and death. Note that for every node, the illness evolves differently based on the probability distribution described in the following subsections.

### 2.3.1 Case fatality ratio

The baseline case fatality ratio (CFR), i.e. the fatality ratio among all positively tested, is assumed 1.38% (CI 1.23-1.53%) [29, 32], similar to the estimate of Shim et al. [33] for South Korea. Dividing deaths-to-date by cases-to-date leads to a biased estimate of CFR, called naive CFR (nCFR) as the delays from confirmation of a case to death is not accounted for, as well as due to under-reporting of cases and even deaths. The reported numbers agree with recently published study for symptomatic case fatality ratio in China [34].

### 2.3.2 Infection fatality, intensive care and hospitalisation ratios

Infection fatality ratio (IFR) estimates are based on the study from Verity et al. [29], which reported IFR of 0.66% with 95% confidence interval 0.4% to 1.3%. These estimates are consistent with IFR on Princess Diamond Cruise ship, when demographic differences are accounted for [35]. In Imperial College report on COVID-19 [36], these numbers have been also adjusted for the non-uniform attack rate and UK demography. The authors obtained age-stratified IFR estimates by

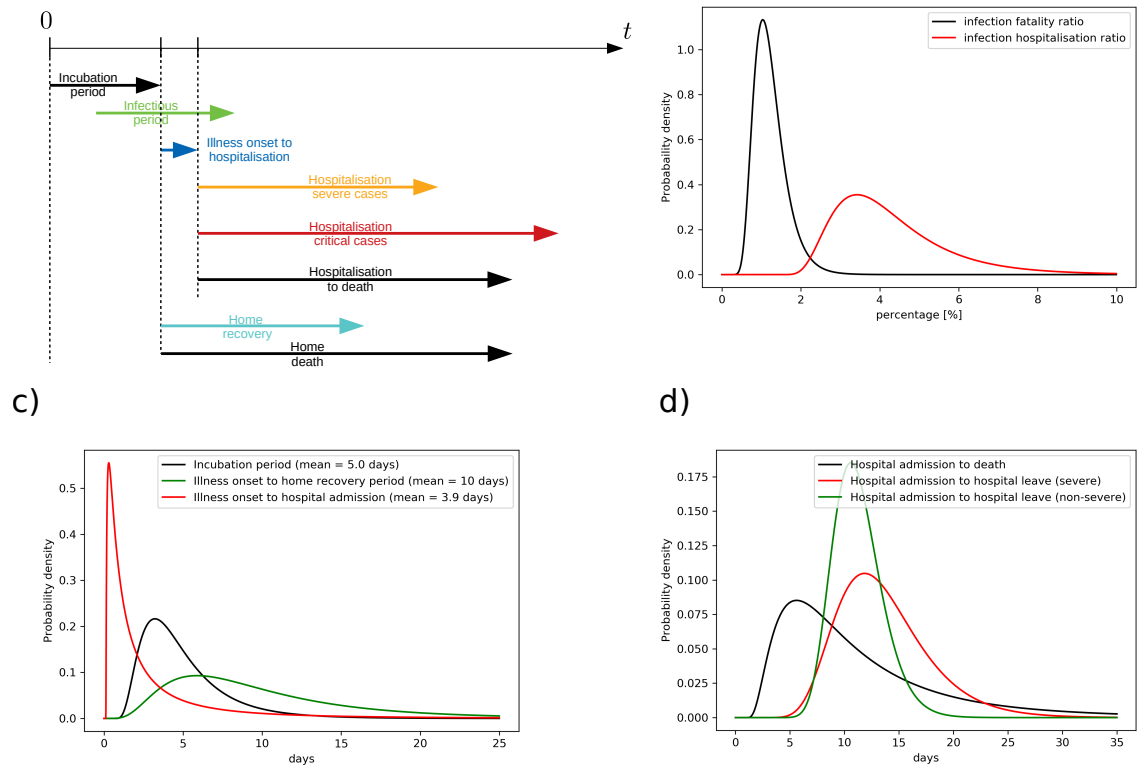


Figure 4: a) A simplified sketch of illness evolution. b) Infection fatality ratio distribution and infection hospitalisation ratio distribution for ensemble simulations. Computed based on data from Verity et al. [29]. c) Incubation period and illness onset to hospitalisation distribution for COVID-19 patients [30]. d) Mean distribution of hospital admission to death, hospital admission to hospital leave for severe and for non-severe illness [30, 31].

adjusting their CFR estimates using COVID-19 prevalence data for expatriates evacuated from Wuhan. This approach involves very large uncertainties. Furthermore, Verity et al. [29] collected data from patients who were hospitalised in Hubei, mainland China, where median age is 37.4 years while median age in Slovenia is 44.5 years. Study reported a strong age gradient in risk of death. We have applied those age-stratified estimates to the Slovenian population. Performing an age-stratified weighted average, we compute the total IFR of 1.16% (CI 0.63-2.22%). Similar total IFR was reported by a comprehensive study for Italy [37] (1.29%, 95% CI 0.89-2.01%). On the other hand Modi et al. [38] have recently estimated somewhat lower IFR (0.95%, 95% CI 0.47-1.70%) with the lower bound of 0.65% for Lombardia, consistent with 0.58% lower bound for Bergamo province. Villa et al. [39] reported a bit higher IFR of 1.6% (95% CI 1.1-2.1%). A more comprehensive meta-analysis of IFR estimates was done by Meyerowitz-Katz and Merone [40].

Analogously, we compute the average hospitalisation rate of 6.37% (95% CI 3.8-13%) based on Verity et al. [29]. Slightly lower age-dependent hospitalisation rates were estimated for COVID-19 patients in USA by Garg et al. [41], which adjusted for demography of Slovenia (but not accounting for non-uniform attack rate) gives hospitalisation rate of 3.97%. The latter result better coincides with the observed number of hospitalisations in Slovenia. No interval estimate is given, thus we use the same relative error as given by Verity et al. [29]. The final hospitalisation rate is thus 3.97% (95% CI 2.37-8.10%). We assume that roughly 1/4-1/3 of all hospitalised cases are admitted to ICU [42], despite some studies showing smaller proportions [43]. We assume that one half of cases admitted to intensive care unit (ICU) are fatal [44].

Taking into account infection fatality ratio, hospitalisation ratio and ICU admission ratio, it follows that roughly one half of all deaths occur at home/elderly care center/palliative care center, which agrees with the present data for Slovenia [45]. Note that for simplicity, we have assumed uniform attack rate across all ages, despite studies showing that working population is most likely to get infected [46, 47]. Using the minimization procedures, we obtain parameters of log-normal distribution which best fits both values and their 95% confidence interval (Fig. 4b).

### 2.3.3 Incubation period - infection to illness onset

Mean incubation period is taken to be 5.0 days (95% CI 4.2-6.0 days), while the 95th percentile of the distribution was 10.6 days (95% CI 8.5-14.1 days) and 99th percentile 15.4 days (99% CI 11.7-22.5 days) [30]. Similar numbers were reported in earlier studies with less patients included [19, 48, 49, 50]. Log-normal distribution is used among for incubation period among nodes. However, the parameters of the lognormal distribution remain fixed due to numerical instability of their computation. Thus, all ensemble members have the same log-normal distribution of incubation period. Incubation period distribution and other outcome parameters are shown in Fig. 4c.

### 2.3.4 Infectious period

The infectious period is not yet well defined. A small study from German cohort of only 9 patients with mild clinical courses [51] showed that viral shedding was high during the first week of symptoms and peaking at day 4. Another study from Singapore reported seven clusters in which virus was transmitted from a COVID-19 patient before experiencing symptoms. According to the authors pre-symptomatic transmission occurred 1-3 days before symptoms onset [52]. We have therefore estimated latent (non-infectious) period of 3 days and infectious period to start 2 days before the completion of incubation period (average incubation period is estimated at 5 days). Thus, we assume 2 days of pre-symptomatic transmission. Slightly larger numbers (2.55 days for Singapore and 2.89 days for Tianjin, China) were reported by Tindale et al. [53].

The infectious period likely ends around 5 days from symptoms onset, so the total period of infectiousness lasts  $T_{bioinf} \approx 7$  days. Note however that none of the interval boundaries are known exactly. Determining its final boundary is especially challenging, as it depends on the social factors as well, e.g. whether the infected cases are able to self-isolate from surroundings and how strictly they follow the self-isolation order. Here, we assume strict (100%) self-isolation and use a *social*



infectious period of  $T_{socioinf} = 5$  days. It starts 2.5 days (95% CI 1.5-3.5 days) after infection and end 2.5 days after incubation (95% CI 1.5-3.5 days) as the case ascertainment typically occurs 2 days after symptoms onset [54]. The infectious period fall in line with study of Bi et al. [28], Fig. S2. It also falls in line with the reported proportion of pre-symptomatic transmission (representing half of infectious period) being 48% for Singapore, 62% for Tianjin, China [55] and 44% for 77 infector-infectee pairs in Gaungzhou, China [56].

## 2.4 Illness onset to hospitalisation or home recovery

From the illness onset on, there are two possible recovery pathways: home recovery or hospitalisation (Fig. 4c). Home recovery period for mild cases has not been documented officially but is reported to be within one and two weeks. Since it does not affect the hospitalisation statistics, we here assume it to be log-normally distributed with mean period of 10 days.

Based on the clinical study of Linton et al. [30], mean illness onset to hospital admission period is 3.9 days (95% CI 2.9-5.3 days), with median of 1.5 days (95% CI 1.2-1.9 days), 5% percentile at 0.2 days (95% CI 0.1-0.3 days) and 95% percentile at 14 days (95% CI 10.3-20.1 days). Only the distribution of data for living patients is accounted for, since we now understand the severity of the illness. In China, fatal cases were admitted to hospital on average two days later [30].

## 2.5 Hospital admission to recovery or death

Hospital admission to death median (mean) length is assumed 6.7 (8.6) days long (Fig. 4d). Only slightly longer periods were reported by Mizumoto and Chowell [57] with mean length of 10.1 days. Hospital admission to recovery is on average longer than hospital admission to death. The median hospitalisation length is 11 days (95% CI 10-13) for non-severe cases and 13 days for severe (95% CI 11-17) [30]. Both are log-normally distributed. For ensemble computations, their medians are further log-normally distributed according to their respective confidence intervals. Similar numbers were reported by Zhou et al. [58] with 11 day (95% CI 7-14) mean hospital length of stay and 8 day (95% CI 4-12) mean ICU length of stay.

Fatality ratio of severe cases in need of intensive care is reported to be around 50%. We assume fatality ratio of severe cases without intensive care to be normally distributed with mean of 90% (95% CI 85-95%). Fatality ratio of severely ill without oxygen is assumed 10% (95% CI 5-15%).

## 2.6 Initial condition

The initial condition for the simulation is defined for March 12, 2020. To that day, there were 131 symptomatic cases who tested positive in Slovenia, 8 days after first positive case, which implies an anomalously low doubling time of  $\tau = 1.23$  days. This number is case specific as there was winter holiday in Slovenia at the end of February and beginning of March. Thus, lots of cases were imported from Northern Italy (including Lombardy). Other studies typically suggest a doubling time of around 5 days (95% CI 4.3 - 6.2) in the initial uncontrolled stage of the epidemic [59]. However, Abbott et al. [60] report smaller values of around 3.5 days in most of Western Europe. Thus, our choice is doubling time of  $T_{double} = 3.5$  days (95% CI 2.5-4.5 days) for the period before March 12.

Different numbers of actually infected people were suggested in the media reports, ranging from 5 to 20 times the number of reported positive cases. Given the average incubation period of 5 days + (2 days for case ascertainment) and doubling period of 3.5 days, factor  $2^{\frac{T_{inc}+2}{T_{double}}} = 4$  applies. Furthermore, the proportion of asymptomatic cases is around 18% based on the data from Diamond Princess Cruise Ship [61] (mostly older people) and around 33% based on the more recent study [62]. Population screening tests from Iceland reported 41.6% of all who tested positive, did not experience any COVID-19 symptoms [63]. Similar asymptomatic ratio (43.2% (95% CI 32.2-54.7%)) was reported also from a screening study conducted for the Italian town Vo [64]. Another study on the homeless population in Boston reported even larger proportion of

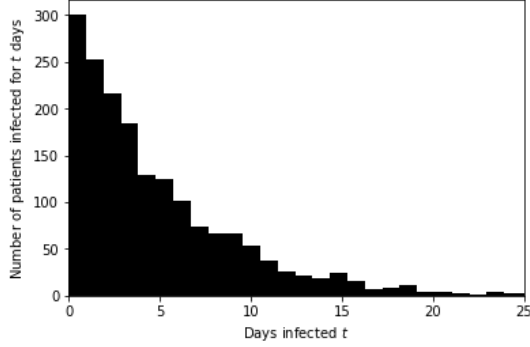


Figure 5: Distribution of 1780 infected people on March 12, 2020, in Slovenia, by the duration of their infection.

asymptomatic cases [65]. The model-driven study of Emery et al. [66] found that 74% (95% CI 70-78%) of SARS-CoV-2 infections proceeded asymptotically, raising also doubts about the IFR. In this study, we opt for 40%, normally distributed with standard deviation of 10%. Furthermore, we double the value to account for the initial under-reporting of symptomatic cases, estimated by Kucharski et al. [17]. All together, this results in almost 1800 infected people in Slovenia by March 12.

Based on the exponential growth in the initial stage of the epidemic and known incubation period, we randomly generate the infection length of the patients with exponential distribution with shape factor of  $T_{double}/\log 2$ , so that 131 develop symptoms and are ascertained by March 12. Initial distribution of 1780 infected people by the time-length of their infection is shown in Fig. 5. Note that in reality, due to many imported cases, the actual infection-time distribution may be slightly different.

## 2.7 Ensemble of simulations

Ensemble of simulations allows to estimate the uncertainty of the epidemic forecasts and to infer confidence in those predictions. There are two levels of perturbations in the ensemble: 1) at the start of each simulation, we perturb parameters, which govern the probability distributions of all model parameters, and 2) each node in the network has its own transmission probability based on its number of contacts and its own disease progression drawn from the associated probability distributions.

The uncertainty is associated with the impact of the intervention-measures on the social network connectivity and the uncertainty attributed to the intrinsic (internal, natural) model uncertainty. The latter can be further divided into:

1. social network uncertainty associated with randomized connections,
2. initial condition uncertainty as random nodes are infected,
3. virus transmission dynamics uncertainty which stems from uncertainty of the parameters, described in Subsection 2.2,
4. disease progression model uncertainty due to uncertainty of the parameters, described in Subsection 2.3.

In Slovenia, the intervention measures were imposed at several time instances between March 13 and March 30 [67]. Their impact was assessed by first perturbing their impact on the social network connectivity and second by using only those members, where the simulated evolution best fits the observed evolution.

The forecast of the COVID-19 epidemic for Slovenia, shown in Section 3, is generated as follows. First, 1000 perturbed simulations were performed. Among all forecasts, only 10% of simulations which best follow the observed number of hospitalised patients on intensive care unit (ICU) and fatal (F) cases are used. The cumulative absolute discrepancy between observed values  $y$  and modeled values  $x$  at time  $t_i$  is measured with a cost function

$$J = \sum_{i=0}^N (|\log y_{ICU}(t_i) - \log x_{ICU}(t_i)| + |\log y_F(t_i) - \log x_F(t_i)|). \quad (5)$$

Logarithms are used to weigh equally the initial and later phase of the pandemic, as the number of infected varies by several orders of magnitude. The described data assimilation approach allow us to estimate both the impact of the intervention measures as well as the changes in the distribution of parameters.

## 2.8 Exclusion experiments

We perform exclusion experiments to assess the contribution of the above mentioned model components uncertainty to the total forecast uncertainty. For example, to estimate the contribution of the randomized social network to the total forecast uncertainty, we run an ensemble of simulations with the same social network, i.e. we exclude the social network perturbation.

The proxy for forecast uncertainty is the relative spread, i.e. the spread of the forecast ensemble, divided by the median value of the forecasts at each time instance. As the spread is approximately symmetric on the logarithmic axis (Fig. 6), we compute the relative spread as:

$$RS(t) = \frac{\log P_{75}(\vec{x}(t)) - \log P_{25}(\vec{x}(t))}{\log \text{median}(\vec{x}(t))}, \quad (6)$$

where  $P_{75}$  and  $P_{25}$  indicate 75th and 25th percentiles of population  $\vec{x}$  at time  $t$ .

## 3 Results

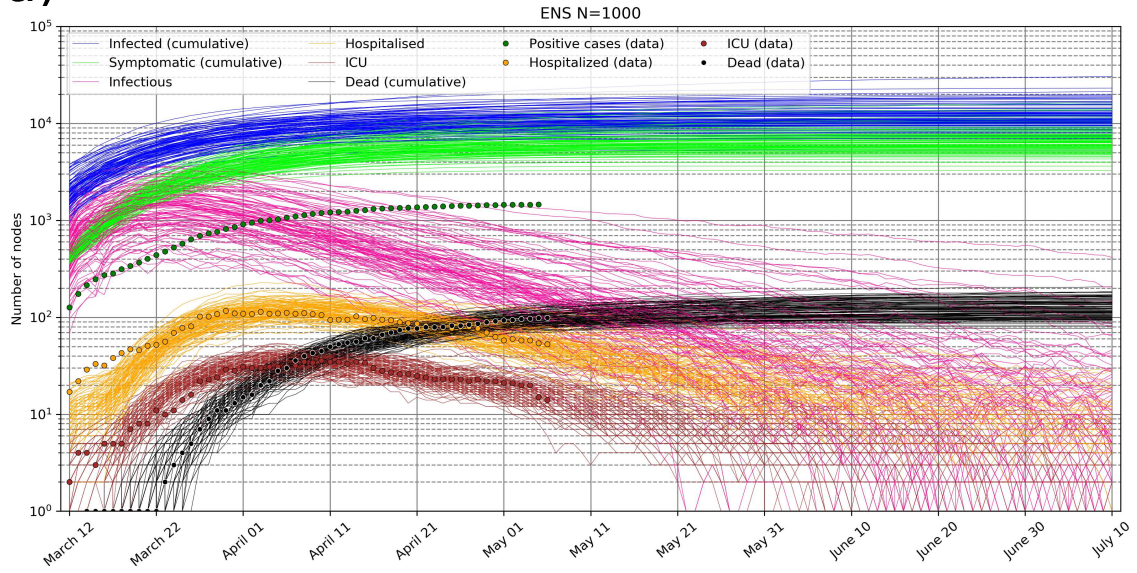
### 3.1 Prediction for Slovenia issued on May 5, 2020

Every day, new data is used to correct the COVID-19 forecast. Fig. 6 shows an example of the ensemble prediction issued on May 5, 2020, simulated from the initial condition on March 12, 2020. The forecast is issued in the already declining stage of the epidemic and assumes ongoing intervention measures. Fig. 6a shows 100 members out of 1000, whose evolution least deviates from the observed data. Fig. 6b shows the associated probabilistic forecast. The infectious population has the largest uncertainty relative to its value, however the number of infectious is not constrained by any measurements. Thus, its relative uncertainty roughly reflects the uncertainty in the hospitalisation, ICU and IFR ratios. The total number of infected to date approaches 11000 people (90% CI 7000-17000), in line with the current estimate of the under-reporting of symptomatic cases (only 17% of cases reported) by Russell et al. [35] and the recently estimated asymptomatic ratio in Italian town of Vo [64].

In April 2020, a National COVID-19 prevalence survey has been completed [68], which reported 1 actively infected out of 1367 tested (0.073% prevalence) and 41 positive for coronavirus antibodies out of 1318 tested (3.1% prevalence, 95% CI 2.2-4%). However, the survey adds very little extra information to better constrain the forecast. First, the number of actively infected is associated with large confidence interval, and second, the antibody tests have significant false-positive rate and varying sensitivity [69].

In the social network model, the current reproduction number  $R$  can be directly measured. For each infectious node, we count the number of nodes it infects. Then we assign the counts to the time instance corresponding to the end of the infectious period. Fig. 7 shows the reproduction number falling below 1 on March 20, 2020, which marks the transition into decaying stage of

a)



b)

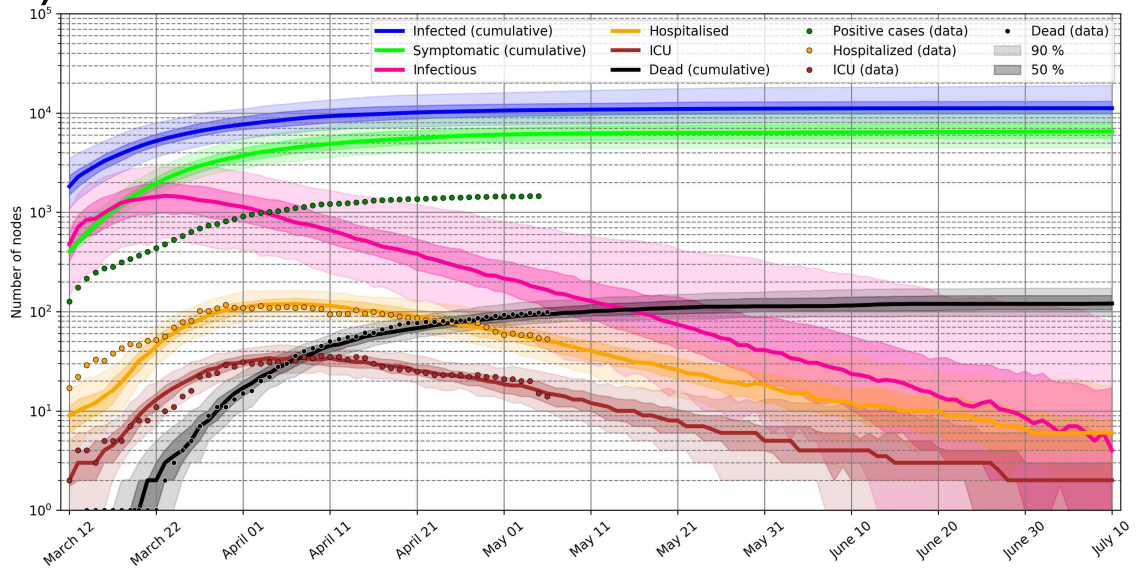


Figure 6: Forecast of COVID-19 pandemic in Slovenia issued on May 5, 2020 and comparison with real data. a) 100 ensemble members which best fit the observed data (dots) are shown. b) Probabilistic forecast: median value, interquartile range (50%; 25th-75th percentile) and 90% range are shown.

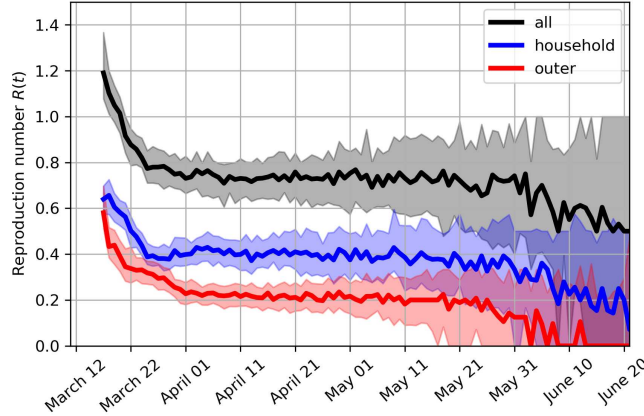


Figure 7: Evolution of the estimated time-varying reproduction number  $R$ , decomposed into reproduction number associated with household transmission and transmission outside households. The shaded regions indicate the interquartile ranges.

the epidemic. Current estimate of  $R$  is at around 0.75, in line with the recent estimate for Slovenia of Manevski et al. [67]. Fig. 7 also shows that the infection is currently much more likely to transmit within households than outside households. If the current intervention measures continue, the reproduction number would start to rapidly decline at the end of May without any extra intervention measures, which indicates effective virus containment when the virus would be transmitted only within some of the household clusters.

The members of the ensemble, which minimize the cost function, can also be used to inverse estimate the posterior distribution of clinical parameters, such as hospitalisation ratio, ICU ratio, ratio of severe infection, and IFR, as well as disease progress parameters such as the probability distribution of the time-span of hospital admission to death. For example, according to Fig. 8a, the true hospitalisation rate is slightly smaller than the first guess, while the infection fatality rate is 0.1% higher in the posterior analysis. As another example, Fig. 8b shows that the posterior estimate of the mean hospital admission to death duration is 7.5 days, half a day longer than the first guess estimate. This inverse technique was also used to estimate the impact of intervention measures on the social network connectivity. However, at the time, virus transmission parameters and some disease progress parameters (e.g. IFR) could not be constrained due to the lack of reliable data on the infectious population and total infected population.

### 3.2 Forecast uncertainty decomposition

Using the exclusion experiments, we evaluated the contribution of different epidemic model components to the total forecast uncertainty of the total number of infected and infectious population. For instance, the ensemble experiment where the social network and the initial condition are fixed (not perturbed) is termed NONET, the experiment without virus transmission dynamics perturbation is called NOTRANS, while the experiment without disease progression model perturbation is named NODIS.

We perform exclusion experiments for two different cases: uncontrolled epidemic and controlled epidemic with intervention measures and low infected population. The results are shown in Fig. 9. We observe, that in the uncontrolled epidemic, the forecast uncertainty is most reduced when the transmission dynamic parameters are not perturbed (experiment NOTRANS in Fig. 9a,b). This also reduces the uncertainty in the epidemic peak and later stages of the epidemic. Fixing disease progression parameters (such as ratio of asymptomatic infections and duration of infectiousness) also significantly reduces uncertainty (experiment NODIS). Fixing initial condition and social network structure reduces the uncertainty only in the initial stage of the epidemic (until around

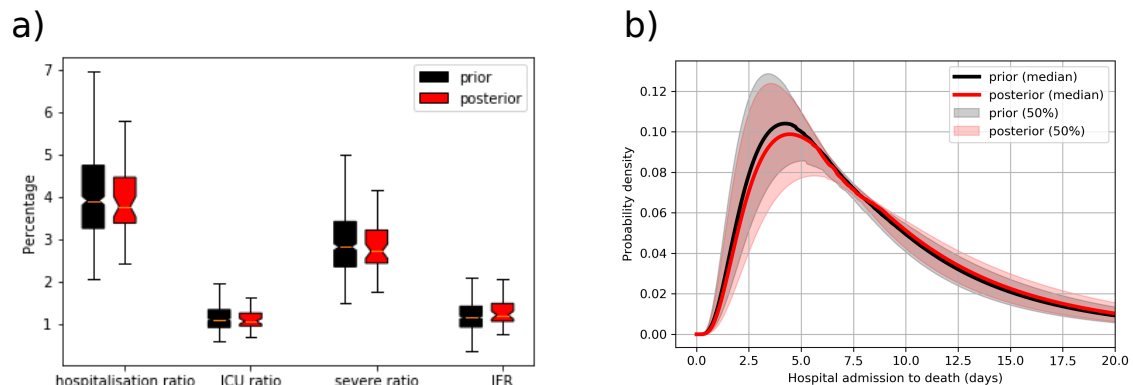


Figure 8: a) Prior and posterior distributions of hospitalisation ratio, intensive care unit (ICU) ratio, ratio of severe symptoms (requiring hospitalisation), and infection fatality ratio (IFR). b) The probability distribution of the duration of hospital admission to death.

day 10), when the number of infected individuals is small (experiment NONET) and homogeneous mixing is an invalid assumption. In the later stage, the uncertainty becomes similar to the basic experiment with all parameters perturbed (experiment ALL). These experiments indicate that the largest contributor to the forecast uncertainty in the uncontrolled epidemic is virus transmission dynamics.

In the controlled epidemic with low number of infected, though, fixing the social network and initial condition (NONET, Fig. 9c) reduces the forecast uncertainty the most (the impact is amplified again in the initial stage), followed by fixing the disease progression parameters, with the impact amplified again in the early part of the simulation. This suggests that the structure of the network and the initial distribution of infected nodes drastically affects the evolution due to heterogeneous mixing and randomized irregular social network. The result suggests that the epidemic forecast can be improved (i.e. its uncertainty decreased) the most by constructing a more realistic model of our social network.

## 4 Discussion, conclusions and further outlook

In this study, we have developed a virus transmission model on the simplified social network of Slovenia with 2 million nodes organised into home/care center clusters. A detailed disease progression model was coupled with the virus transmission model. The model probabilistic prediction is regularly updated on Sledilnik webpage [45] and is occasionally communicated to the Expert Group that provides support to the Government of the Republic of Slovenia for the containment and control of the COVID-19.

We have developed a data assimilation procedure, which minimizes the cost function measuring the deviation from observed ICU, hospitalisation and fatality numbers. The procedure constrains the forecast trajectories closer to the observed values. It also constrains the model parameters. Our approach mimics the established variational data assimilation approach in Numerical Weather Prediction (NWP) [70, 71]. Another example of data assimilation utilisation in epidemiology is by Shaman and Karspeck [72], who used an Ensemble Adjustment Kalman Filter [73].

An indispensable part of the prediction is its uncertainty. In this study, we evaluated the contribution of the virus transmission uncertainty (e.g. reproduction number and its derivatives), network and initial condition uncertainty and uncertainty of the disease progress model to the total uncertainty of the epidemic forecast. We found that in the uncontrolled epidemic, the intrinsic uncertainty mostly originates from the uncertainty of the virus transmission. In the controlled epidemic with low infected population, the randomness of the social network becomes the major source of forecast uncertainty. We also show, that the uncertainty of the forecast and the associated

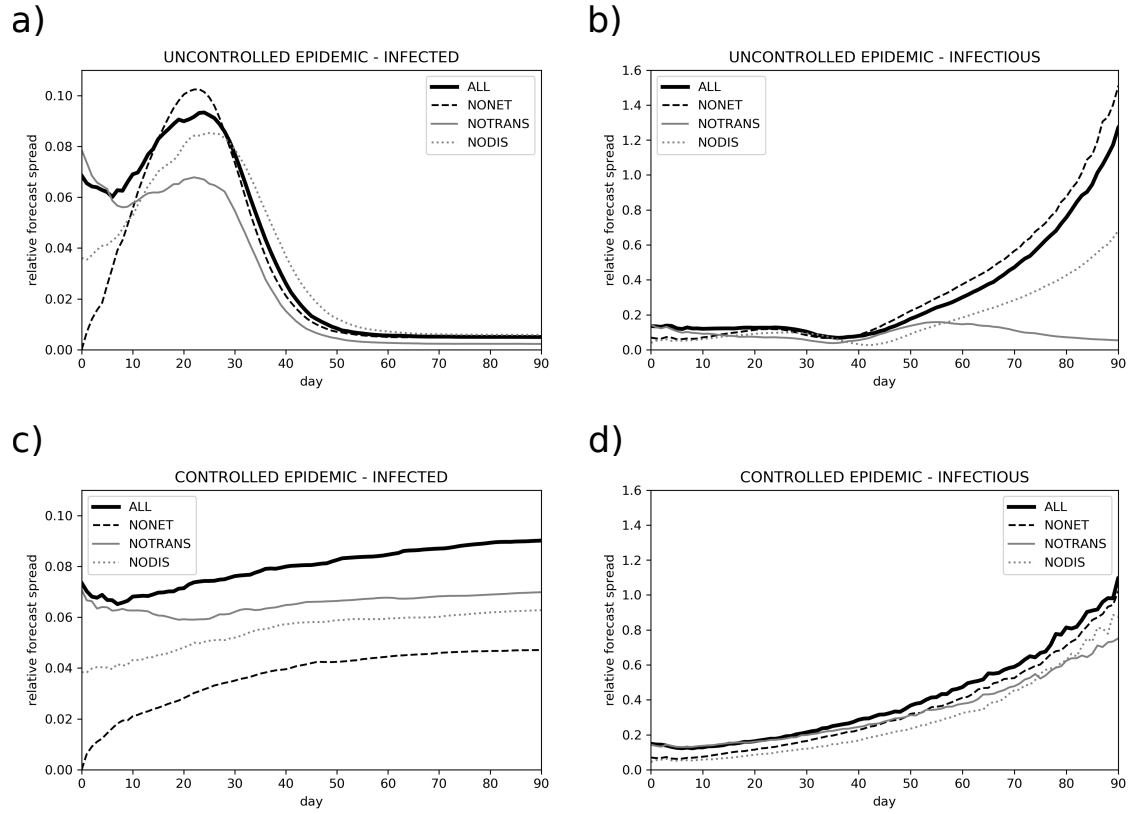


Figure 9: Relative forecast spread, measured by Eq. 6, for uncontrolled epidemic (a,b) and controlled epidemic with low number of infected (c,d), as shown in Fig. 6. The basic experiment with all parameters perturbed is termed ALL. NONET stands for no social network and initial condition perturbation, NOTRANS stands for no transmission dynamics parameters perturbations, while NODIS means no disease progress model parameters perturbations.

risk is extremely asymmetric (roughly symmetric on a logarithmic axis) with long exponential tails, reaching a similar conclusion to the recent study of Petropoulos and Makridakis [74].

There are some limitations of our model which reduce its predictive ability and its usefulness to simulate the impact of intervention measures in advance. The social network model is too simplified, and its average clustering too low. For example regional, work/education clustering based on work/education mobility data is not included in the present social network. The nodes do not have attributions such as age, sex or employment status and the social mixing data [11, 75, 76, 47] is not accounted for yet. Given the high attack rate within households, the social mixing within households is of special importance, thus it is also vital to include the age-distribution of the residents of different household sizes. A more sophisticated treatment of the secondary attack rate is also needed, for example the infectiousness could be modeled as a function of time [56]. Further work should alleviate some of the mentioned limitations to allow more robust simulation of the intervention measures.

The ongoing COVID-19 epidemic has revealed a major gap in our ability to forecast the evolution of the epidemic. No operational center for infectious disease prediction, similar to those employed for the weather predictions (e.g. European Centre for Medium-Range Forecasts or National Center for Environmental Prediction), exists, despite the gigantic societal, economical and health impact of the ongoing epidemic. While the epidemic dynamics is governed by the human social behaviour and its modeling arguably messier than weather forecasting [77], a coordinated modeling effort which borrows the established methods used for Numerical Weather Prediction (NWP) would likely improve our prediction [72]. Accurate models of the real-world social networks are needed to realistically simulate the virus transmission dynamics. Similarly to NWP models [78], the real-time clinical patient data, mobility data [79] and connectivity data (obtained by e.g. postprocessing the bluetooth-generated anonymous contact data [80]), should be rapidly assimilated into the virus spread prognostic model [e.g. 81] to evaluate the changes in contact patterns [82]. This would allow 1) to estimate the critical virus spread parameters and their uncertainty, 2) to forecast the evolution of the epidemic more accurately and based on that forecasts, 3) to implement optimal worldwide-concerted measures to minimize the virus spread. We should be ready for the next big pandemic!

## Acknowledgments

The authors are grateful to Aleks Jakulin, Miha Kadunc (Sinergise), Luka Renko (founder of the volunteer-led Sledilnik.org project) for providing the timely COVID-19 pandemics data for Slovenia. Žiga Zaplotnik would like to thank prof. Alojz Kodre and asis. prof. Simon Čopar (both University of Ljubljana, Faculty of Mathematics and Physics, UL-FMF) for introducing him the node-based analysis of the information spread. We thank fellow physicists Nejc Davidovič and Jan Bohinec (Gen-I) for fruitful discussions as well as asis. prof. Samo Drobne (University of Ljubljana, Faculty of civil and geodetic engineering) for providing the mobility data for Slovenia. Arthur Breitman (Tezos) is thanked for an interesting question on the properties of the virus transmission dynamics related to superspreaders, which initiated further research. Special thanks go to prof. Roman Jerala (National Institute of Chemistry) and prof. Tomaž Zwitter (UL-FMF) for discussions of the model, and for reading and commenting the early manuscript draft as well as for providing useful literature. Finally, Žiga Zaplotnik would like to thank his postdoc supervisor prof. dr. Nedjeljka Žagar (University of Hamburg) for always supporting work beneficial to society.

## References

- [1] William Ogilvy Kermack and A. G. McKendrick. A contribution to the mathematical theory of epidemics. *Proceedings of the Royal Society of London. Series A, Containing Papers of a Mathematical and Physical Character*, 115(772):700–721, aug 1927. ISSN 0950-1207. doi: 10.1098/rspa.1927.0118.



- [2] Herbert W Hethcote. The Mathematics of Infectious Diseases \*. Technical Report 4, 2000. URL <http://www.siam.org/journals/sirev/42-4/37190.html>.
- [3] M. S. Bartlett. Measles Periodicity and Community Size. *Journal of the Royal Statistical Society. Series A (General)*, 120(1):48, 1957. ISSN 00359238.
- [4] J. O. Lloyd-Smith, S. J. Schreiber, P. E. Kopp, and W. M. Getz. Superspreading and the effect of individual variation on disease emergence. *Nature*, 438(7066):355–359, nov 2005. ISSN 14764687. doi: 10.1038/nature04153.
- [5] S. Eubank, C. Barrett, R. Beckman, K. Bisset, L. Durbeck, C. Kuhlman, B. Lewis, A. Marathe, M. Marathe, and P. Stretz. Detail in network models of epidemiology: Are we there yet? *Journal of Biological Dynamics*, 4(5):446–455, sep 2010. ISSN 17513758. doi: 10.1080/17513751003778687.
- [6] M. Elizabeth Halloran, Ira M. Longini, Azhar Nizam, and Yang Yang. Containing bioterrorist smallpox. *Science*, 298(5597):1428–1432, nov 2002. ISSN 00368075. doi: 10.1126/science.1074674.
- [7] Danilo Dolenc. Vsaka peta dvostarševska družina je zunajzakonska skupnost, 2018. URL <https://www.stat.si/StatWeb/News/Index/7725>.
- [8] Lada A. Adamic, Rajan M. Lukose, Amit R. Puniyani, and Bernardo A. Huberman. Search in power-law networks. *Physical Review E - Statistical Physics, Plasmas, Fluids, and Related Interdisciplinary Topics*, 64(4):8, sep 2001. ISSN 1063651X. doi: 10.1103/PhysRevE.64.046135.
- [9] Joseph Norman, Yaneer Bar-Yam, and Nicholas Taleb. Systemic Risk of Pandemic via Novel Pathogens-Coronavirus: A Note. Technical report, 2020.
- [10] Kathy Leung, Mark Jit, Eric H.Y. Lau, and Joseph T. Wu. Social contact patterns relevant to the spread of respiratory infectious diseases in Hong Kong. *Scientific Reports*, 7(1):1–12, aug 2017. ISSN 20452322. doi: 10.1038/s41598-017-08241-1.
- [11] Joël Mossong, Niel Hens, Mark Jit, Philippe Beutels, Kari Auranen, Rafael Mikolajczyk, Marco Massari, Stefania Salmaso, Gianpaolo Scalia Tomba, Jacco Wallinga, Janneke Heijne, Malgorzata Sadkowska-Todys, Magdalena Rosinska, and W. John Edmunds. Social contacts and mixing patterns relevant to the spread of infectious diseases. *PLoS Medicine*, 5(3):0381–0391, mar 2008. ISSN 15491277. doi: 10.1371/journal.pmed.0050074.
- [12] S. Y. Del Valle, J. M. Hyman, H. W. Hethcote, and S. G. Eubank. Mixing patterns between age groups in social networks. *Social Networks*, 29(4):539–554, oct 2007. ISSN 03788733. doi: 10.1016/j.socnet.2007.04.005.
- [13] Leon Danon, Ashley P Ford, Thomas House, Chris P Jewell, Matt J Keeling, Gareth O Roberts, Joshua V Ross, and Matthew C Vernon. Networks and the Epidemiology of Infectious Disease. *Interdisciplinary Perspectives on Infectious Diseases*, 2011:284909, 2011. ISSN 1687-708X. doi: 10.1155/2011/284909. URL <https://doi.org/10.1155/2011/284909>.
- [14] Jonathan M Read, Ken T.D Eames, and W. John Edmunds. Dynamic social networks and the implications for the spread of infectious disease. *Journal of The Royal Society Interface*, 5(26):1001–1007, sep 2008. ISSN 1742-5689. doi: 10.1098/rsif.2008.0013. URL <https://royalsocietypublishing.org/doi/10.1098/rsif.2008.0013>.
- [15] Ying Liu, Albert A Gayle, Annelies Wilder-Smith, and Joacim Rocklöv. The reproductive number of COVID-19 is higher compared to SARS coronavirus. *Journal of Travel Medicine*, 2020:1–4, 2020. doi: 10.1093/jtm/taaa021. URL <https://academic.oup.com/jtm/article-abstract/27/2/taaa021/5735319>.

- [16] Jonathan M Read, Jessica R E Bridgen, Derek A T Cummings, Antonia Ho, and Chris P Jewell. Novel coronavirus 2019-nCoV: early estimation of epidemiological parameters and epidemic predictions. *medRxiv preprint*, 2020. doi: 10.1101/2020.01.23.20018549. URL <https://doi.org/10.1101/2020.01.23.20018549>.
- [17] Adam J. Kucharski, Timothy W. Russell, Charlie Diamond, Yang Liu, John Edmunds, Sebastian Funk, Rosalind M. Eggo, Fiona Sun, Mark Jit, James D. Munday, Nicholas Davies, Amy Gimma, Kevin van Zandvoort, Hamish Gibbs, Joel Hellewell, Christopher I. Jarvis, Sam Clifford, Billy J. Quilty, Nikos I. Bosse, Sam Abbott, Petra Klepac, and Stefan Flasche. Early dynamics of transmission and control of COVID-19: a mathematical modelling study. *The Lancet Infectious Diseases*, 0(0), 2020. ISSN 14744457. doi: 10.1016/S1473-3099(20)30144-4.
- [18] Joseph T. Wu, Kathy Leung, and Gabriel M. Leung. Nowcasting and forecasting the potential domestic and international spread of the 2019-nCoV outbreak originating in Wuhan, China: a modelling study. *The Lancet*, 395(10225):689–697, feb 2020. ISSN 1474547X. doi: 10.1016/S0140-6736(20)30260-9.
- [19] Qun Li, Xuhua Guan, Peng Wu, Xiaoye Wang, Lei Zhou, Yeqing Tong, Ruiqi Ren, Kathy S.M. Leung, Eric H.Y. Lau, Jessica Y. Wong, Xuesen Xing, Nijuan Xiang, Yang Wu, Chao Li, Qi Chen, Dan Li, Tian Liu, Jing Zhao, Man Liu, Wenxiao Tu, Chuding Chen, Lianmei Jin, Rui Yang, Qi Wang, Suhua Zhou, Rui Wang, Hui Liu, Yinbo Luo, Yuan Liu, Ge Shao, Huan Li, Zhongfa Tao, Yang Yang, Zhiqiang Deng, Boxi Liu, Zhitao Ma, Yanping Zhang, Guoqing Shi, Tommy T.Y. Lam, Joseph T. Wu, George F. Gao, Benjamin J. Cowling, Bo Yang, Gabriel M. Leung, and Zijian Feng. Early Transmission Dynamics in Wuhan, China, of Novel Coronavirus-Infected Pneumonia. *New England Journal of Medicine*, jan 2020. ISSN 0028-4793. doi: 10.1056/nejmoa2001316.
- [20] Mingwang Shen, Zhihang Peng, Yanni Xiao, and Lei Zhang. Modelling the epidemic trend of the 2019 novel coronavirus outbreak in China. *bioRxiv*, page 2020.01.23.916726, jan 2020. doi: 10.1101/2020.01.23.916726.
- [21] Maimuna Majumder and Kenneth D. Mandl. Early Transmissibility Assessment of a Novel Coronavirus in Wuhan, China. *SSRN Electronic Journal*, jan 2020. doi: 10.2139/ssrn.3524675.
- [22] Shi Zhao, Qianyin Lin, Jinjun Ran, Salihu S. Musa, Guangpu Yang, Weiming Wang, Yijun Lou, Daozhou Gao, Lin Yang, Daihai He, and Maggie H. Wang. Preliminary estimation of the basic reproduction number of novel coronavirus (2019-nCoV) in China, from 2019 to 2020: A data-driven analysis in the early phase of the outbreak. *International Journal of Infectious Diseases*, 92:214–217, mar 2020. ISSN 18783511. doi: 10.1016/j.ijid.2020.01.050.
- [23] Natsuko Imai, Anne Cori, Ilaria Dorigatti, Marc Baguelin, Christl A Donnelly, Steven Riley, and Neil M Ferguson. Report 3: Transmissibility of 2019-nCoV. Technical report. URL <https://doi.org/10.25561/77148>.
- [24] Biao Tang, Xia Wang, Qian Li, Nicola Luigi Bragazzi, Sanyi Tang, Yanni Xiao, and Jianhong Wu. Estimation of the Transmission Risk of the 2019-nCoV and Its Implication for Public Health Interventions. *Journal of Clinical Medicine*, 9(2):462, feb 2020. ISSN 2077-0383. doi: 10.3390/jcm9020462.
- [25] WHO. Report of the WHO-China Joint Mission on Coronavirus Disease 2019 (COVID-19). Technical report, 2020. URL [https://www.who.int/publications-detail/report-of-the-who-china-joint-mission-on-coronavirus-disease-2019-\(covid-19\)](https://www.who.int/publications-detail/report-of-the-who-china-joint-mission-on-coronavirus-disease-2019-(covid-19)).
- [26] Yang Liu, Rosalind M Eggo, and Adam J Kucharski. Secondary attack rate and superspreading events for SARS-CoV-2. *The Lancet*, 395(10227):e47, mar 2020. ISSN 0140-6736. doi: 10.1016/S0140-6736(20)30462-1.

- [27] Rachel M. Burke, Claire M. Midgley, Alissa Dratch, Marty Fenstersheib, Thomas Haupt, Michelle Holshue, Isaac Ghinai, M. Claire Jarashow, Jennifer Lo, Tristan D. McPherson, Sara Rudman, Sarah Scott, Aron J. Hall, Alicia M. Fry, and Melissa A. Rolfes. Active Monitoring of Persons Exposed to Patients with Confirmed COVID-19 — United States, January–February 2020. *MMWR. Morbidity and Mortality Weekly Report*, 69(9):245–246, mar 2020. ISSN 0149-2195. doi: 10.15585/mmwr.mm6909e1. URL [http://www.cdc.gov/mmwr/volumes/69/wr/mm6909e1.htm?s\\_cid=mm6909e1\\_w](http://www.cdc.gov/mmwr/volumes/69/wr/mm6909e1.htm?s_cid=mm6909e1_w).
- [28] Qifang Bi, Yongsheng Wu, Shujiang Mei, Chenfei Ye, Xuan Zou, Zhen Zhang, Xiaojian Liu, Lan Wei, Shaun A Truelove, Tong Zhang, Wei Gao, Cong Cheng, Xiujuan Tang, Xiaoliang Wu, Yu Wu, Binbin Sun, Suli Huang, Yu Sun, Juncen Zhang, Ting Ma, Justin Lessler, and Teijian Feng. Epidemiology and Transmission of COVID-19 in Shenzhen China: Analysis of 391 cases and 1,286 of their close contacts. *medRxiv*, page 2020.03.03.20028423, mar 2020. doi: 10.1101/2020.03.03.20028423.
- [29] Robert Verity, Lucy C Okell, Ilaria Dorigatti, Peter Winskill, Charles Whittaker, Natsuko Imai, Gina Cuomo-dannenburg, Hayley Thompson, Patrick G T Walker, Han Fu, Amy Dighe, Jamie T Griffin, Marc Baguelin, Sangeeta Bhatia, Adhiratha Boonyasiri, Anne Cori, Zulma Cucunubá, Rich Fitzjohn, Katy Gaythorpe, Will Green, Arran Hamlet, Wes Hinsley, Daniel Laydon, Gemma Nedjati-gilani, Steven Riley, Sabine Van Elsland, Erik Volz, Haowei Wang, Yuanrong Wang, Xiaoyue Xi, Christl A Donnelly, Azra C Ghani, and Neil M Ferguson. Estimates of the severity of coronavirus disease 2019 : a model-based analysis. *Lancet Infectious Diseases*, 3099(20):1–9, 2020. doi: 10.1016/S1473-3099(20)30243-7.
- [30] Natalie M Linton, Tetsuro Kobayashi, Yichi Yang, Katsuma Hayashi, Andrei R Akhmetzhanov, Sung-Mok Jung, Baoyin Yuan, Ryo Kinoshita, and Hiroshi Nishiura. Incubation Period and Other Epidemiological Characteristics of 2019 Novel Coronavirus Infections with Right Truncation: A Statistical Analysis of Publicly Available Case Data. *Journal of clinical medicine*, 9(2), feb 2020. ISSN 2077-0383. doi: 10.3390/jcm9020538. URL <http://www.ncbi.nlm.nih.gov/pubmed/32079150>.
- [31] Wei-jie Guan, Zheng-yi Ni, Yu Hu, Wen-hua Liang, Chun-quan Ou, Jian-xing He, Lei Liu, Hong Shan, Chun-liang Lei, David S.C. Hui, Bin Du, Lan-juan Li, Guang Zeng, Kwok-Yung Yuen, Ru-chong Chen, Chun-li Tang, Tao Wang, Ping-yan Chen, Jie Xiang, Shi-yue Li, Jin-lin Wang, Zi-jing Liang, Yi-xiang Peng, Li Wei, Yong Liu, Ya-hua Hu, Peng Peng, Jian-ming Wang, Ji-yang Liu, Zhong Chen, Gang Li, Zhi-jian Zheng, Shao-qin Qiu, Jie Luo, Chang-jiang Ye, Shao-yong Zhu, and Nan-shan Zhong. Clinical Characteristics of Coronavirus Disease 2019 in China. *New England Journal of Medicine*, feb 2020. ISSN 0028-4793. doi: 10.1056/nejmoa2002032.
- [32] Timothy W. Russell, Joel Hellewell, Sam Abbott, Christopher I Jarvis, Kevin van Zandvoort, Ruwan Ratnayake, Working Group CMMID NCov, Stefan Flasche, Rosalind Eggo, John Edmunds, and Adam J Kucharski. Using a delay-adjusted case fatality ratio to estimate under-reporting — CMMID Repository, 2020. URL [https://cmmid.github.io/topics/covid19/severity/global\\_cfr\\_estimates.html](https://cmmid.github.io/topics/covid19/severity/global_cfr_estimates.html).
- [33] Eunha Shim, Kenji Mizumoto, Wongyeong Choi, and Gerardo Chowell. Estimating the risk of COVID-19 death during the course of the outbreak in Korea, February–March, 2020. *medRxiv*, page 2020.03.30.20048264, apr 2020. doi: 10.1101/2020.03.30.20048264.
- [34] Joseph T. Wu, Kathy Leung, Mary Bushman, Nishant Kishore, Rene Niehus, Pablo M. de Salazar, Benjamin J. Cowling, Marc Lipsitch, and Gabriel M. Leung. Estimating clinical severity of COVID-19 from the transmission dynamics in Wuhan, China. *Nature Medicine*, pages 1–5, mar 2020. ISSN 1078-8956. doi: 10.1038/s41591-020-0822-7. URL <http://www.nature.com/articles/s41591-020-0822-7>.

- [35] Timothy W Russell, Joel Hellewell, Christopher I Jarvis, Kevin van Zandvoort, Sam Abbott, Ruwan Ratnayake, Stefan Flasche, Rosalind M Eggo, W John Edmunds, and Adam J Kucharski. Estimating the infection and case fatality ratio for coronavirus disease (COVID-19) using age-adjusted data from the outbreak on the Diamond Princess cruise ship, February 2020. *Eurosurveillance*, 25(12):2000256, mar 2020. ISSN 1560-7917. doi: 10.2807/1560-7917.ES.2020.25.12.2000256. URL <https://www.eurosurveillance.org/content/10.2807/1560-7917.ES.2020.25.12.2000256>.
- [36] Neil M Ferguson, Daniel Laydon, Gemma Nedjati-Gilani, Natsuko Imai, Kylie Ainslie, Marc Baguelin, Sangeeta Bhatia, Adhiratha Boonyasiri, Zulma Cucunubá, Gina Cuomo-Dannenburg, Amy Dighe, Ilaria Dorigatti, Han Fu, Katy Gaythorpe, Will Green, Arran Hamlet, Wes Hinsley, Lucy C Okell, Sabine Van Elsland, Hayley Thompson, Robert Verity, Erik Volz, Haowei Wang, Yuanrong Wang, Patrick Gt Walker, Caroline Walters, Peter Winskill, Charles Whittaker, Christl A Donnelly, Steven Riley, and Azra C Ghani. Impact of non-pharmaceutical interventions (NPIs) to reduce COVID-19 mortality and healthcare demand. *COVID-19 Reports*, 9, 2020. doi: 10.25561/77482. URL <https://doi.org/10.25561/77482>.
- [37] Gianluca Rinaldi and Matteo Paradisi. An empirical estimate of the infection fatality rate of COVID-19 from the first Italian outbreak. *medRxiv*, page 2020.04.18.20070912, apr 2020. doi: 10.1101/2020.04.18.20070912.
- [38] Chirag Modi, Vanessa Boehm, Simone Ferraro, George Stein, and Uros Seljak. Total COVID-19 Mortality in Italy: Excess Mortality and Age Dependence through Time-Series Analysis. *medRxiv*, page 2020.04.15.20067074, apr 2020. doi: 10.1101/2020.04.15.20067074. URL <http://medrxiv.org/content/early/2020/04/20/2020.04.15.20067074.1.abstract>.
- [39] Matteo Villa, James F. Myers, and Federico Turkheimer. COVID-19: Recovering estimates of the infected fatality rate during an ongoing pandemic through partial data. *medRxiv*, page 2020.04.10.20060764, apr 2020. doi: 10.1101/2020.04.10.20060764. URL <https://www.medrxiv.org/content/10.1101/2020.04.10.20060764v1>.
- [40] Gideon Meyerowitz-Katz and Lea Merone. A systematic review and meta-analysis of published research data on COVID-19 infection-fatality rates. *medRxiv*, page 2020.05.03.20089854, may 2020. doi: 10.1101/2020.05.03.20089854.
- [41] Shikha Garg, Lindsay Kim, Michael Whitaker, Alissa O’Halloran, Charisse Cummings, Rachel Holstein, Mila Prill, Shua J. Chai, Pam D. Kirley, Nisha B. Alden, Breanna Kawasaki, Kimberly Yousey-Hindes, Linda Niccolai, Evan J. Anderson, Kyle P. Openo, Andrew Weigel, Maya L. Monroe, Patricia Ryan, Justin Henderson, Sue Kim, Kathy Como-Sabetti, Ruth Lynfield, Daniel Sosin, Salina Torres, Alison Muse, Nancy M. Bennett, Laurie Billing, Melissa Sutton, Nicole West, William Schaffner, H. Keipp Talbot, Clarissa Aquino, Andrea George, Alicia Budd, Lynnette Brammer, Gayle Langley, Aron J. Hall, and Alicia Fry. Hospitalization Rates and Characteristics of Patients Hospitalized with Laboratory-Confirmed Coronavirus Disease 2019 — COVID-NET, 14 States, March 1–30, 2020. *MMWR. Morbidity and Mortality Weekly Report*, 69(15):458–464, apr 2020. ISSN 0149-2195. doi: 10.15585/mmwr.mm6915e3. URL [http://www.cdc.gov/mmwr/volumes/69/wr/mm6915e3.htm?s{}\\_cid=mm6915e3{}\\_w](http://www.cdc.gov/mmwr/volumes/69/wr/mm6915e3.htm?s{}_cid=mm6915e3{}_w).
- [42] Stephanie Bialek, Ellen Boundy, Virginia Bowen, Nancy Chow, Amanda Cohn, Nicole Downing, Sascha Ellington, Ryan Gierke, Aron Hall, Jessica MacNeil, Priti Patel, Georgina Peacock, Tamara Pilishvili, Hilda Razzaghi, Nia Reed, Matthew Ritchey, and Erin Sauber-Schatz. Severe Outcomes Among Patients with Coronavirus Disease 2019 (COVID-19) — United States, February 12–March 16, 2020. *MMWR. Morbidity and Mortality Weekly Report*, 69(12):343–346, mar 2020. ISSN 0149-2195. doi: 10.15585/mmwr.mm6912e2. URL [http://www.cdc.gov/mmwr/volumes/69/wr/mm6912e2.htm?s{}\\_cid=mm6912e2{}\\_w](http://www.cdc.gov/mmwr/volumes/69/wr/mm6912e2.htm?s{}_cid=mm6912e2{}_w).
- [43] Nancy Chow, Katherine Fleming-Dutra, Ryan Gierke, Aron Hall, Michelle Hughes, Tamara Pilishvili, Matthew Ritchey, Katherine Roguski, Tami Skoff, and Emily Ussery. Preliminary

estimates of the prevalence of selected underlying health conditions among patients with coronavirus disease 2019 - United States, February 12-March 28, 2020, apr 2020. ISSN 1545861X.

- [44] ICNARC. ICNARC report on COVID-19 in critical care. Technical report, Intensive care national adult & research centre, 2020. URL <https://www.icnarc.org/About/Latest-News/2020/04/04/Report-On-2249-Patients-Critically-Ill-With-Covid-19>.
- [45] Luka Renko, Miha Kadunc, and Aleks Jakulin. COVID-19 Sledilnik, 2020. URL <https://covid-19.sledilnik.org/{#}/stats>.
- [46] Kenji Mizumoto, Ryosuke Omori, and Hiroshi Nishiura. Age specificity of cases and attack rate of novel coronavirus disease (COVID-19). *medRxiv*, page 2020.03.09.20033142, mar 2020. doi: 10.1101/2020.03.09.20033142.
- [47] Nicholas G Davies, Petra Klepac, Yang Liu, Kiesha Prem, Mark Jit, and Rosalind M Eggo. Age-dependent effects in the transmission and control of COVID-19 epidemics. *medRxiv*, page 2020.03.24.20043018, mar 2020. doi: 10.1101/2020.03.24.20043018. URL <http://medrxiv.org/content/early/2020/03/27/2020.03.24.20043018.abstract>.
- [48] Tao Liu, Jianxiong Hu, Min Kang, Lifeng Lin, Haojie Zhong, Jianpeng Xiao, Guanhao He, Tie Song, Qiong Huang, Zuhua Rong, Aiping Deng, Weilin Zeng, Xiaohua Tan, Siqing Zeng, Zhihua Zhu, Jiansen Li, Donghua Wan, Jing Lu, Huihong Deng, Jianfeng He, and Wenjun Ma. Time-varying transmission dynamics of Novel Coronavirus Pneumonia in China. *bioRxiv*, page 2020.01.25.919787, jan 2020. doi: 10.1101/2020.01.25.919787. URL <https://www.biorxiv.org/content/10.1101/2020.01.25.919787v1>.
- [49] Stephen A. Lauer, Kyra H. Grantz, Qifang Bi, Forrest K. Jones, Qulu Zheng, Hannah R. Meredith, Andrew S. Azman, Nicholas G. Reich, and Justin Lessler. The Incubation Period of Coronavirus Disease 2019 (COVID-19) From Publicly Reported Confirmed Cases: Estimation and Application. *Annals of Internal Medicine*, mar 2020. ISSN 0003-4819. doi: 10.7326/m20-0504.
- [50] Moritz U. G. Kraemer, Chia-Hung Yang, Bernardo Gutierrez, Chieh-Hsi Wu, Brennan Klein, David M. Pigott, Louis du Plessis, Nuno R. Faria, Ruoran Li, William P. Hanage, John S. Brownstein, Maylis Layan, Alessandro Vespignani, Huaiyu Tian, Christopher Dye, Oliver G. Pybus, and Samuel V. Scarpino. The effect of human mobility and control measures on the COVID-19 epidemic in China. *Science*, page eabb4218, mar 2020. ISSN 0036-8075. doi: 10.1126/science.abb4218.
- [51] Roman Woelfel, Victor Max Corman, Wolfgang Guggemos, Michael Seilmaier, Sabine Zange, Marcel A Mueller, Daniela Niemeyer, Patrick Vollmar, Camilla Rothe, Michael Hoelscher, Tobias Bleicker, Sebastian Bruenink, Julia Schneider, Rosina Ehmann, Katrin Zwirgmaier, Christian Drosten, and Clemens Wendtner. Clinical presentation and virological assessment of hospitalized cases of coronavirus disease 2019 in a travel-associated transmission cluster. *medRxiv*, page 2020.03.05.20030502, mar 2020. doi: 10.1101/2020.03.05.20030502.
- [52] Wycliffe E. Wei, Zongbin Li, Calvin J. Chiew, Sarah E. Yong, Matthias P. Toh, and Vernon J. Lee. Presymptomatic Transmission of SARS-CoV-2 — Singapore, January 23–March 16, 2020. *MMWR. Morbidity and Mortality Weekly Report*, 69(14):411–415, apr 2020. ISSN 0149-2195. doi: 10.15585/mmwr.mm6914e1. URL [http://www.cdc.gov/mmwr/volumes/69/wr/mm6914e1.htm?s\\_cid=mm6914e1\\_w](http://www.cdc.gov/mmwr/volumes/69/wr/mm6914e1.htm?s_cid=mm6914e1_w).
- [53] Lauren Tindale, Michelle Coombe, Jessica E Stockdale, Emma Garlock, Wing Yin Venus Lau, Manu Saraswat, Yen-Hsiang Brian Lee, Louxin Zhang, Dongxuan Chen, Jacco Wallinga, and Caroline Colijn. Transmission interval estimates suggest pre-symptomatic spread of COVID-19. *medRxiv*, (February):2020.03.03.20029983, mar 2020. doi: 10.1101/2020.03.03.20029983.

- [54] R. Moss, J. Wood, D. Brown, F. Shearer, A.J. Black, Cheng A.C., J.M. McCaw, and J. McVernon. Modelling the impact of COVID-19 in Australia to inform transmission reducing measures and health system preparedness. Technical report, Doherty Institute, University of Melbourne, 2020. URL [https://www.doherty.edu.au/uploads/content{}\\_doc/McVernon{}\\_Modelling{}\\_COVID-19{}\\_07Apr1{}\\_with{}\\_appendix.pdf](https://www.doherty.edu.au/uploads/content{}_doc/McVernon{}_Modelling{}_COVID-19{}_07Apr1{}_with{}_appendix.pdf).
- [55] Tapiwa Ganyani, Cecile Kremer, Dongxuan Chen, Andrea Torneri, Christel Faes, Jacco Wallinga, and Niel Hens. Estimating the generation interval for COVID-19 based on symptom onset data. *medRxiv*, page 2020.03.05.20031815, mar 2020. doi: 10.1101/2020.03.05.20031815.
- [56] Xi He, Eric H. Y. Lau, Peng Wu, Xilong Deng, Jian Wang, Xinxin Hao, Yiu Chung Lau, Jessica Y. Wong, Yajuan Guan, Xinghua Tan, Xiaoneng Mo, Yanqing Chen, Baolin Liao, Weilie Chen, Fengyu Hu, Qing Zhang, Mingqiu Zhong, Yanrong Wu, Lingzhai Zhao, Fuchun Zhang, Benjamin J. Cowling, Fang Li, and Gabriel M. Leung. Temporal dynamics in viral shedding and transmissibility of COVID-19. *Nature Medicine*, pages 1–4, apr 2020. ISSN 1078-8956. doi: 10.1038/s41591-020-0869-5. URL <http://www.nature.com/articles/s41591-020-0869-5>.
- [57] Kenji Mizumoto and Gerardo Chowell. Estimating Risk for Death from 2019 Novel Coronavirus Disease, China, January–February 2020. *Emerging Infectious Diseases*, 26(6), jun 2020. ISSN 1080-6040. doi: 10.3201/eid2606.200233.
- [58] Fei Zhou, Ting Yu, Ronghui Du, Guohui Fan, Ying Liu, Zhibo Liu, Jie Xiang, Yeming Wang, Bin Song, Xiaoying Gu, Lulu Guan, Yuan Wei, Hui Li, Xudong Wu, Jiuyang Xu, Shengjin Tu, Yi Zhang, Hua Chen, and Bin Cao. Clinical course and risk factors for mortality of adult inpatients with COVID-19 in Wuhan, China: a retrospective cohort study. *The Lancet*, 0(0), mar 2020. ISSN 01406736. doi: 10.1016/s0140-6736(20)30566-3.
- [59] Luca Ferretti, Chris Wymant, Michelle Kendall, Lele Zhao, Anel Nurtay, Lucie Abeler-Dörner, Michael Parker, David Bonsall, and Christophe Fraser. Quantifying SARS-CoV-2 transmission suggests epidemic control with digital contact tracing. *Science (New York, N.Y.)*, mar 2020. ISSN 1095-9203. doi: 10.1126/science.abb6936. URL <http://www.ncbi.nlm.nih.gov/pubmed/32234805>.
- [60] Sam Abbott, Joel Hellewell, James D Munday, June Young Chun, Robin N. Thompson, Nikos I Bosse, Yung-Wai Desmond Chan, Timothy W Russell, Christopher Jarvis, Stefan Flasche, Adam J Kucharski, Rosalind Eggo, and Sebastian Funk. Temporal variation in transmission during the COVID-19 outbreak — CMMID Repository, 2020. URL <https://cmmid.github.io/topics/covid19/current-patterns-transmission/global-time-varying-transmission.html>.
- [61] Kenji Mizumoto, Katsushi Kagaya, Alexander Zarebski, and Gerardo Chowell. Estimating the asymptomatic proportion of coronavirus disease 2019 (COVID-19) cases on board the Diamond Princess cruise ship, Yokohama, Japan, 2020. *Eurosurveillance*, 25(10):2000180, mar 2020. ISSN 1560-7917. doi: 10.2807/1560-7917.es.2020.25.10.2000180.
- [62] Hiroshi Nishiura, Tetsuro Kobayashi, Takeshi Miyama, Ayako Suzuki, Sungmok Jung, Katsuma Hayashi, Ryo Kinoshita, Yichi Yang, Baoyin Yuan, Andrei R Akhmetzhanov, and Natalie M Linton. Estimation of the asymptomatic ratio of novel coronavirus (2019-nCoV) infections among passengers on evacuation flights, feb 2020.
- [63] Daniel F. Gudbjartsson, Agnar Helgason, Hakon Jonsson, Olafur T. Magnusson, Pall Melsted, Gudmundur L. Norddahl, Jona Saemundsdottir, Asgeir Sigurdsson, Patrick Sulem, Arna B. Agustsdottir, Berglind Eirisdottir, Run Fridriksdottir, Elisabet E. Gardarsdottir, Gudmundur Georgsson, Olafia S. Gretarsdottir, Kjartan R. Gudmundsson, Thora R. Gunnarsdottir, Arnaldur Gylfason, Hilma Holm, Brynjar O. Jensson, Aslaug Jonasdottir, Frosti Jonsson, Kamilla S. Josefsdottir, Thordur Kristjansson, Droplaug N. Magnúsdottir,

- Louise le Roux, Gudrun Sigmundsdottir, Gardar Sveinbjornsson, Kristin E. Sveinsdottir, Maney Sveinsdottir, Emil A. Thorarensen, Bjarni Thorbjornsson, Arthur Löve, Gisli Masson, Ingileif Jonsdottir, Alma D. Möller, Thorolfur Gudnason, Karl G. Kristinsson, Unnur Thorsteinsdottir, and Kari Stefansson. Spread of SARS-CoV-2 in the Icelandic Population. *New England Journal of Medicine*, page NEJMoa2006100, apr 2020. ISSN 0028-4793. doi: 10.1056/NEJMoa2006100. URL <http://www.nejm.org/doi/10.1056/NEJMoa2006100>.
- [64] Enrico Lavezzo, Elisa Franchin, Constanze Ciavarella, Gina Cuomo-Dannenburg, Luisa Barzon, Claudia Del Vecchio, Lucia Rossi, Riccardo Manganelli, Arianna Loregian, Nicolò Navarin, Davide Abate, Manuela Sciro, Stefano Merigliano, Ettore Decanale, Maria Cristina Vanuzzo, Francesca Saluzzo, Francesco Onelia, Monia Pacenti, Saverio Parisi, Giovanni Carretta, Daniele Donato, Luciano Flor, Silvia Cocchio, Giulia Masi, Alessandro Sperduti, Lorenzo Cattarino, Renato Salvador, Katy A.M. Gaythorpe, Imperial College London COVID-19 Response Team, Alessandra R Brazzale, Stefano Toppo, Marta Trevisan, Vincenzo Baldo, Christl A. Donnelly, Neil M. Ferguson, Ilaria Dorigatti, and Andrea Crisanti. Suppression of COVID-19 outbreak in the municipality of Vo, Italy. *medRxiv*, page 2020.04.17.20053157, apr 2020. doi: 10.1101/2020.04.17.20053157.
- [65] Travis P. Baggett, Harrison Keyes, Nora Sporn, and Jessie M. Gaeta. COVID-19 outbreak at a large homeless shelter in Boston: Implications for universal testing. *medRxiv*, page 2020.04.12.20059618, apr 2020. doi: 10.1101/2020.04.12.20059618.
- [66] Jon C Emery, Timothy W Russell, Yang Liu, Joel Hellewell, Carl AB Pearson, nCoV Working group, Gwenan M Knight, Rosalind M Eggo, Adam J Kucharski, Sebastian Funk, Stefan Flasche, Rein M G J Houben, Katherine E Atkins, Petra Klepac, Akira Endo, Christopher I Jarvis, Nicholas G Davies, Eleanor M Rees, Sophie R Meakin, Alicia Rosello, Kevin van Zandvoort, James D Munday, W John Edmunds, Thibaut Jombart, Megan Auzenberg, Emily S Nightingale, Mark Jit, Sam Abbott, David Simons, Nikos I Bosse, Quentin J Leclerc, Simon R Procter, C Julian Villabona-Arenas, Damien C Tully, Arminder K Deol, Fiona Yueqian Sun, Stéphane Hué, Anna M Foss, Kiesha Prem, Graham Medley, Amy Gimma, Rachel Lowe, Samuel Clifford, Matthew Quaife, Charlie Diamond, Hamish P Gibbs, and Billy J Quilty. The contribution of asymptomatic SARS-CoV-2 infections to transmission—a model-based analysis of the Diamond Princess outbreak. Technical report, 2020.
- [67] Damjan Manevski, PhD Maja Pohar Perme, and Rok Blagus. Ocena stopnje reprodukcije okužbe in deleža okuženih z virusom SARS-CoV-2 v Sloveniji. *Slovenian Medical Journal*, 89:1–12, apr 2020. ISSN 1581-0224. doi: 10.6016/ZDRAVVESTN.3068.
- [68] National COVID-19 prevalence survey — GOV.SI. URL <https://www.gov.si/en/news/2020-04-24-national-covid-19-prevalence-survey/>.
- [69] Ria Lassaunière, Anders Frische, Zitta B Harboe, Alex CY Nielsen, Anders Fomsgaard, Karen A Krogfelt, and Charlotte S Jørgensen. Evaluation of nine commercial SARS-CoV-2 immunoassays. *medRxiv*, page 2020.04.09.20056325, apr 2020. doi: 10.1101/2020.04.09.20056325.
- [70] Eugenia Kalnay. *Atmospheric modeling, data assimilation, and predictability*, volume 54. 2003. ISBN 9780521791793. doi: 10.1256/00359000360683511.
- [71] William A. Lahoz and Philipp Schneider. Data assimilation: making sense of Earth Observation. *Frontiers in Environmental Science*, 2(May):1–28, 2014. ISSN 2296-665X. doi: 10.3389/fenvs.2014.00016. URL <http://journal.frontiersin.org/article/10.3389/fenvs.2014.00016/abstract>.
- [72] Jeffrey Shaman and Alicia Karspeck. Forecasting seasonal outbreaks of influenza. *Proceedings of the National Academy of Sciences of the United States of America*, 109(50):20425–20430, dec 2012. ISSN 00278424. doi: 10.1073/pnas.1208772109.

- [73] Jeffrey L. Anderson. An Ensemble Adjustment Kalman Filter for Data Assimilation. *Monthly Weather Review*, 129(12):2884–2903, 2001. ISSN 0027-0644. doi: 10.1175/1520-0493(2001)129<2884:AEAKFF>2.0.CO;2.
- [74] Fotios Petropoulos and Spyros Makridakis. Forecasting the novel coronavirus COVID-19. *PLOS ONE*, 15(3):e0231236, mar 2020. ISSN 1932-6203. doi: 10.1371/journal.pone.0231236. URL <https://dx.plos.org/10.1371/journal.pone.0231236>.
- [75] Sebastian Meyer and Leonhard Held. Incorporating social contact data in spatio-temporal models for infectious disease spread. *Biostatistics (Oxford, England)*, 18(2):338–351, 2017. ISSN 1468-4357. doi: 10.1093/biostatistics/kxw051. URL <http://www.ncbi.nlm.nih.gov/pubmed/28025182><http://www.pubmedcentral.nih.gov/articlerender.fcgi?artid=PMC5379927>.
- [76] Kiesha Prem, Alex R. Cook, and Mark Jit. Projecting social contact matrices in 152 countries using contact surveys and demographic data. *PLoS Computational Biology*, 13(9), sep 2017. ISSN 15537358. doi: 10.1371/journal.pcbi.1005697.
- [77] Kelly R Moran, Geoffrey Fairchild, Nicholas Generous, Kyle Hickmann, Dave Osthus, Reid Priedhorsky, James Hyman, and Sara Y Del Valle. Epidemic Forecasting is Messier Than Weather Forecasting: The Role of Human Behavior and Internet Data Streams in Epidemic Forecast. *The Journal of Infectious Diseases*, 214(S4):404–408, 2016. doi: 10.1093/infdis/jiw375. URL [https://academic.oup.com/jid/article-abstract/214/suppl\\_4/S404/2527912](https://academic.oup.com/jid/article-abstract/214/suppl_4/S404/2527912).
- [78] Peter Bauer, Alan Thorpe, and Gilbert Brunet. The quiet revolution of numerical weather prediction, sep 2015. ISSN 14764687.
- [79] Marta C. González, César A. Hidalgo, and Albert-László Barabási. Understanding individual human mobility patterns. *Nature*, 453(7196):779–782, jun 2008. ISSN 14764687. doi: 10.1038/nature06958.
- [80] Raj Dandekar, Shane G Henderson, Marijn Jansen, Sarat Moka, Yoni Nazarathy, Christopher Rackauckas, Peter G Taylor, and Aapeli Vuorinen. Safe Blues: A Method for Estimation and Control in the Fight Against COVID-19. Technical report, 2020. URL <https://safeblues.org/>.
- [81] Zhidong Cao, Qingpeng Zhang, Xin Lu, Dirk Pfeiffer, Lei Wang, Hongbing Song, Tao Pei, Zhongwei Jia, and Daniel Dajun Zeng. Incorporating Human Movement Data to Improve Epidemiological Estimates for 2019-nCoV. *medRxiv*, page 2020.02.07.20021071, feb 2020. doi: 10.1101/2020.02.07.20021071. URL <http://medrxiv.org/content/early/2020/02/09/2020.02.07.20021071.abstract>.
- [82] Juanjuan Zhang, Maria Litvinova, Yuxia Liang, Yan Wang, Wei Wang, Shanlu Zhao, Qianhui Wu, Stefano Merler, Cécile Viboud, Alessandro Vespignani, Marco Ajelli, and Hongjie Yu. Changes in contact patterns shape the dynamics of the COVID-19 outbreak in China. *Science*, page eabb8001, may 2020. ISSN 0036-8075. doi: 10.1126/science.abb8001. URL <https://www.sciencemag.org/lookup/doi/10.1126/science.abb8001>.